

1 **Splitting of Concrete Cover in Steel Fiber Reinforced Concrete:**
2 **Semi-Empirical Modelling and Minimum Confinement Requirements.**

3
4 **E. García-Taengua^{1*}, J.R. Martí-Vargas², P. Serna³**

5 ¹ School of Planning, Architecture and Civil Engineering, Queen's University, Belfast,
6 Northern Ireland, United Kingdom.

7 ²⁻³ ICITECH-Institute of Concrete Science and Technology, Universitat Politècnica de
8 València, Valencia, Spain

9 **e-mail addresses:** e.garcia-taengua@qub.ac.uk, jrmarti@cst.upv.es, pserna@cst.upv.es

10 ***Corresponding author:** e.garcia-taengua@qub.ac.uk

11
12 **ABSTRACT**

13 The use of steel fiber reinforced concrete (SFRC) is becoming more and more common.
14 Concerning bond of rebars to concrete, fibers provide passive confinement and not only
15 improve bond performance but also affect the mode of bond failure. To analyze these
16 aspects, a series of prismatic specimens have been subjected to the Pull Out Test, and an
17 accurate model for predicting the mode of bond failure has been developed. The
18 following factors have been considered: concrete compressive strength (30-50 MPa),
19 rebar diameter (8-20 mm), concrete cover (between 30 mm and 5 times rebar diameter),
20 fiber content (up to 70 kg/m³), and fiber slenderness and length. This model relates
21 splitting probability to the factors considered. It has been proved that increasing fiber
22 content restrains the risk of splitting failure. The favorable effect of fibers when
23 preventing splitting failures has been revealed to be more important for higher concrete
24 compressive strength values, which require higher concrete cover/diameter ratios for
25 splitting failure to be prevented. Fiber slenderness and fiber length modify the effect of
26 fiber content on splitting probability and therefore on minimum cover/diameter ratios
27 required to prevent splitting failures.

28
29 **KEYWORDS:**

30 concrete, fiber, confinement, splitting, bond, model, failure

34 **1. INTRODUCTION**

35 This section describes the phenomena involved in bond of rebars to concrete and
36 reviews previous literature concerned with the role of fibers. For a better understanding,
37 this information is organised in three different subsections. The first one presents an
38 overview of the mechanisms controlling bond of rebars to concrete. Then, the second
39 subsection deals with the different modes of bond failure and puts splitting failures in
40 context, paying special attention to the role of passive confinement. Finally, the role of
41 fibers in relation to bond and specially splitting failures is exposed. All this information
42 contextualizes the topic under study and justifies the objectives of this study, which are
43 detailed right after that.

44

45 **1.1 Bond of Reinforcing Bars to Concrete**

46 Bond between reinforcement and concrete is commonly conceptualized as a shear stress,
47 or bond stress, distributed over the surface of the rebar along the embedded length.
48 Bond stress can be defined as the ratio between the rate of change in axial force along
49 the rebar and the area of rebar surface over which this change takes place [1]. However,
50 there are other aspects besides bond stress to be considered, especially in the case of
51 deformed, ribbed rebars [1–3], mainly related to radial stresses.

52 As Figure 1 shows, the tensile load pulling the rebar out of concrete produces reaction
53 forces which are exerted on the surrounding concrete by ribs. These reactions can be
54 decomposed in two components and therefore, the bond phenomenon involves: a) a
55 shear component, parallel to the rebar axis, so that there are triaxially compressed
56 concrete regions in front of each rib, and b) a radial component, orthogonal to the shear
57 component, which extends bond mechanisms to the surrounding concrete.

58 As the axial load on the rebar increases, the wedging action by rebar ribs increases and
59 concrete between ribs is crushed. At the same time, the derived radial stresses are also
60 increased and concrete tensile strength is reached in the surrounding concrete. This
61 leads to the phenomenon of transverse microcracking which is at the very basis of the
62 loss of strain compatibility between rebar and concrete: relative displacement of the
63 rebar with respect to concrete (slip) increases as a result of the widening of these
64 microcracks.

65 Progress of the rebar slip implies activation of bond and progressive increase of bond
66 stresses until the bond strength is reached. Bond stress–slip curves are characterized by

67 postpeak softening behavior: bond stress remains remarkable even at very large slips in
68 the postpeak region [4], and slippage represents shear fracture [5].
69 Consequently, because of both shear and radial components, and based on confinement
70 conditions, bond failure can occur in two different major modes. One mode consists in
71 splitting of concrete surrounding the rebar (splitting failure), and the other mode
72 consists in having the rebar pulled out after the shear failure of the steel-concrete
73 interface (pullout failure).

74

75 **1.2 Modes of Bond Failure and Passive Confinement**

76 Confinement plays a major role as a parameter affecting bond. A distinction is made
77 between active and passive confinement. Active confinement is the consequence of
78 concrete being compressed by external forces, for instance reactions in supports or
79 beam-column joints. Passive confinement is the constraining effect that results from
80 concrete cover and transverse reinforcement. This constraining effect is progressively
81 activated with the onset of bond stresses.

82 Splitting failures occur when concrete is not well confined. Transverse cracks originated
83 at the rebar-concrete interface may eventually reach concrete surface, and if there is no
84 transverse reinforcement capable of bearing the derived tensile stresses, bond capacity
85 is totally lost in a brittle failure followed by a considerable slippage.

86 Pullout failures, on the other hand, occur when confinement prevents these cracks from
87 reaching concrete surface. The concrete crushed between ribs, which defines a
88 cylindrical frictional surface around the rebar [6], is extracted with the rebar. After the
89 shearing has progressed over the entire length of embedment of the rebar, the force
90 drops and then the remaining pullout is resisted only by friction.

91 Passive confinement includes not only the effect of concrete cover but also that of
92 transverse reinforcement, and is treated in similar ways by different codes. The major
93 concern regarding passive confinement is connected to the minimum values of
94 transverse reinforcement or concrete cover in order to prevent concrete splitting [7].
95 According to the Model Code [8], concrete is considered well confined when concrete
96 cover is not less than five times the rebar diameter. The minimum concrete cover value
97 to avoid splitting failures is approximately between 2.5 and 3.0 times rebar diameter [9,
98 10].

99 The confining effect of concrete cover is most usually typified by rebar diameter:
100 concrete cover/diameter ratio is the reference parameter, because the effect of concrete

101 cover is inversely related to rebar diameter. Passive confinement affects bond
102 performance in terms of bond strength and bond failure ductility as well [7], not only in
103 relation to the mode of bond failure [11, 12]. Furthermore, bond stress–slip curves
104 become steeper as concrete cover increases (FIB 2000): concrete confinement in the
105 splice/development region improves the ductility of bond failure as well [13].

106

107 **1.3 Bond of Reinforcing Bars to Steel Fiber Reinforced Concrete (SFRC)**

108 Fibers have a positive effect on bond of reinforcement to concrete, even when low fiber
109 contents are considered [14]. Fibers improve bond performance because they confine
110 reinforcement (playing a similar role to that of the transverse reinforcement) and
111 because they broaden the range of crack width values within which passive confinement
112 remains active [14–16]. Improvements in bond performance of concrete are really
113 important in terms of toughness and ductility of the material [13, 17].

114 In particular, the Spanish code for structural concrete [18] explicitly states that fibers
115 improve bond capacity of concrete and that this can be taken into account when
116 designing anchors and splices. Similar statements are found in the recommendations by
117 other organisms [10, 19].

118 However, the positive effect of fibers is acknowledged but is not always explicitly
119 introduced in formulations for anchorage/splice lengths. Considering that the use of
120 non-conventional concretes, including steel fiber reinforced concrete (SFRC hereafter),
121 is becoming more and more common [20–22], it is likely that anchorage lengths are
122 higher than necessary in most of the cases. How to take advantage of the higher
123 ductility and energy absorption capacity of SFRC to reduce anchorage lengths when
124 using fibers is not a straightforward issue. In this sense, several studies have been
125 performed attempting to model the bond phenomenon and anchorage behavior in
126 general [23–30].

127 A central issue is whether the effect of fibers on bond is modified by concrete
128 compressive strength and rebar diameter. Since large diameters increase the tendency to
129 concrete cover splitting, an important issue is the study of the relationship between the
130 presence of fibers and the concrete cover needed to prevent splitting failures. In fact, the
131 effect of fibers on bond when there is splitting of the concrete cover proves to be very
132 important [25, 31]. On the contrary, it is not so clearly significant when splitting does
133 not occur: under such circumstances fibers have been reported to affect bond failure
134 ductility but not bond strength.

135 The study how fibers determine mode of bond failure, and how they are related to
136 concrete compressive strength and rebar diameter in terms of probability that no cover
137 splitting occurs are issues that have not been addressed in scientific literature yet.

138

139 **2. OBJECTIVES**

140 The main objectives of this research have been:

- 141 • Deepening the knowledge of the phenomena involved in bond of reinforcement
142 to Steel Fiber Reinforced Concrete (SFRC), especially regarding the role of
143 fibers in relation to cover splitting and its prevention.
- 144 • Studying the effect of fiber geometry, fiber content, concrete compressive
145 strength, and rebar diameter on minimum concrete cover values needed to
146 prevent splitting failures.
- 147 • Obtaining analytical expressions which prove useful to estimate the risk or
148 probability of splitting of the concrete cover in terms of the factors considered.
- 149 • Using the aforementioned analytical expressions to predict minimum
150 confinement requirements that have to be met to avoid cover splitting on bond
151 failure.

152

153 **3. EXPERIMENTAL PROGRAMME**

154

155 **3.1 Factors and Levels Considered**

156 The factors considered have been: concrete compressive strength (f_c), rebar diameter
157 (D), concrete cover (C), steel fiber content (C_f), and fiber geometry (slenderness (λ_f)
158 and length (l_f)).

159 The values or levels considered for each one of these factors are summarized in Table 1.
160 To consider concrete compressive strength, three different reference mixes with
161 compressive strength values between 30MPa and 50 MPa have been included. Each one
162 of them has led to a group of different mixes as a result of adding fibers. Since they
163 have been produced and tested sequentially, they have been numbered accordingly: all
164 type I mixes were produced and tested in a first stage, then all type II mixes, and finally
165 all type III mixes. They differ in terms of water/cement ratio, maximum aggregate size,
166 and cement content, since this research is focused on normal strength concrete. The
167 three reference mix designs considered in this research are summarized in Table 2.

168 Four different rebar diameters have been considered. 8mm rebars have been considered
169 as representative of small rebars used in real applications (6mm and 8mm for building,
170 8mm and 10mm for civil engineering works). 16mm rebars have been selected because
171 they are a commonplace in bond literature. At first (series with type I mixes) 20mm
172 rebars were tested in addition to 8mm and 16mm diameters. However, after this first
173 series, considering 8-12-16 mm diameters seemed more convenient than 8-16-20 mm.
174 That is the reason why the values considered for rebar diameters are the same for type II
175 and type III series but they differ from those for type I series (Table 3).

176 Concrete cover values have been defined as a function of rebar diameter. C1 is the
177 smallest concrete cover value: in the first stage (type I series) it was 30 mmn, which is
178 the minimum acceptable according to the Spanish code [18]. However, it was reset to
179 2.5 times the rebar diameter for type II and type III series, because this is usually
180 assumed as the boundary distinguishing splitting failures and pullout failures. C3 is 5
181 times the rebar diameter in all cases, because this is the situation that the Model Code
182 [8] defines as 'good confinement'. C2 was an intermediate value, $C1 < C2 < C3$: for type I
183 series it was the average of C1 and C3, but for type II and type III series it was
184 redefined as 3.5 times the rebar diameter.

185 Four types of hooked-end steel fibers have been considered which are different in terms
186 of slenderness and length only: 45/50, 65/60, 80/35, and 80/50. They all are within the
187 so-called macro-fibers and among the ones which are most widely used in precast
188 industry.

189 Fiber contents considered have been decided below 1% in volume fraction (V_f) in
190 addition to unreinforced concrete (0 kg/m^3), fiber contents from 40 kg/m^3 ($V_f = 0.51\%$)
191 to $60\text{-}70 \text{ kg/m}^3$ ($V_f = 0.76\text{-}0.89\%$) constitute the referential frame for most usual SFRC
192 applications.

193

194 **3.2 Materials**

195 Cement type CEM II/B-M 42.5 R was used in all cases. The aggregates used have been
196 river sand, crushed limestone coarse aggregate, and limestone filler. The
197 superplasticizer used has been a polycarboxylate ether. The reinforcing bars were type
198 B 500 S. With respect to the steel fibers used, all of them are cold-drawn, hooked-end
199 fibers made with low carbon steel (yield strength 1100 MPa minimum) and without any
200 coating.

201 Each one of these reference mix designs was initially tested and adjusted to admit a
202 volume fraction of 0.5% of 65/60 fibers with slump values between 10 cm and 15 cm.
203 However, each one of these reference mix designs would be different in each particular
204 case since fiber type and fiber content would differ according to their having been
205 defined as factors. Consequently, filler and admixture amounts were adjusted in each
206 case to keep slump values between 10 cm and 15 cm at the same time segregation was
207 prevented.

208

209 **3.3 Pull Out Test**

210 A modified version of the Pull Out Test (POT) has been selected as the most
211 appropriate test for the purposes of this research. Specimens for the POT have been
212 designed based on the RILEM recommendations [32–34] which prescribes the
213 following requirements: a) total length of the specimen (L) is to be 10 times the rebar
214 diameter, though never less than 200 mm; and b) embedded length (L') is to be 5 times
215 the rebar diameter, where the absence of sleeve protection allows the generation of bond
216 stresses between rebar and concrete.

217 These conditions have been observed in all POT specimens produced and tested.

218 Preliminary calculations following Eurocode 2 (art. 8.4.2) [35] were made in order to
219 avoid rebar yielding so that specimens failure could be related only to bond failure in all
220 cases.

221 Specimens cross-section was defined as a function of rebar diameter and therefore
222 varies depending on that parameter and on the concrete cover value considered in each
223 particular case. Cross-section of POT specimens is sketched in Figure 3 in terms of the
224 diameter of the rebar (D), the side (S), and the factor 'concrete cover', variable (C). As
225 shown in Figure 3, rebar is positioned excentrically so that the factor 'concrete cover' is
226 restricted to two out of four semi-axes in the cross-section. With respect to the other two
227 semi-axes, concrete cover had to be greater in order to have a good confinement.
228 According to the Model Code [8], it has a good confinement with concrete cover values
229 bigger than 5 times the rebar diameter. It has been taken as reference a rebar diameter of
230 25 mm so that further research with bigger rebar diameters is compatible with all data
231 obtained and reported herein. Accordingly, for the two semi-axes not considered as
232 variable within the cross-section, a minimum dimension of $5 \cdot 25 = 125$ mm was
233 established.

234

235 **3.4 Design of the Experiment**

236 In this case, a total of 5 factors (f_c , D , C , C_f , λ_f) is under consideration, each one of
237 them at 3 different values.

238 The selection of specimens to be produced and tested has followed a highly fractioned
239 factorial plan [36] so that reliable, statistically sound conclusions can be obtained from
240 experimental results after a reasonable number of tests.

241 The consideration given to concrete compressive strength as a factor is somewhat
242 different with respect to how other factors have been handled when planning the
243 experiment. It was more convenient to organize the highly fractioned factorial plan
244 independently of concrete compressive strength, and then producing and testing all
245 these combinations for type I series first, then for type II series, and then for type III
246 series. The result is a fractional factorial design organized in blocks.

247 The combinations tested for each series resulting from the reference mixes are shown in
248 Table 3. Each one of these combinations consisted of 3 POT specimens and 2
249 cylindrical specimens produced with concrete from the same batch. The number of POT
250 specimens produced and tested is $9 \times 3 = 27$ for each series, and since there are 3 series,
251 the total number of POT specimens in this research has been $27 \times 3 = 81$, far less than
252 the 729 specimens that a complete experiment would have required.

253

254 **3.5 Experimental methods**

255 All concrete mixes in this research have been produced by following the same process
256 and sequence in all cases.

257 Right after mixing, concrete slump was measured according to the standard EN 12350-
258 2:2006. The criterion established for fresh mixes was that slump values ranged between
259 10 cm and 15 cm. Then, the concrete used was poured back to the mixer, and after 1
260 more minute mixing, POT specimens and cylindrical specimens were cast.

261 Each one of the batches of concrete produced was characterized by testing under
262 compression the two cylindrical specimens produced simultaneously with POT
263 specimens. All cylindrical specimens were tested at the same age POT specimens were
264 tested, i.e. 28 days. Test method to determine compressive strength was carried out
265 according to EN 12390-2:2009.

266 Pull out tests were carried out as shown in Figure 4. The specimen to be tested was
267 supported by a rigid steel plate with a hole in its center to allow the rebar passing
268 through. The lower end of the rebar was anchored by clamps. By operating a hydraulic

269 system the supporting plate was pulled up and, as a result, the rebar was pulled out of
270 the specimen.

271 The slip of the rebar was monitored on the surface opposite to that from which the rebar
272 was being pulled out by means of a LVDT sensor. It was located on this surface in order
273 to detect the load corresponding to the onset of bond stress along the entire embedded
274 length.

275

276 **4. RESULTS**

277

278 **4.1 Concrete compressive strength**

279 Concrete compressive strength average values obtained for type I, type II, and type III
280 mixes were 32 MPa, 48 MPa, and 44 MPa respectively, obtained from cylindrical
281 specimens tested at the age of 28 days. These average values have been used for the
282 analysis of the results presented in following sections. The coefficient of variation has
283 been 8.5%, 11% and 10.8%, respectively.

284

285 **4.2 Mode of failure and bond strength**

286 Table 3 shows the experimental results obtained, namely: the number of specimens out
287 of each set of three that experienced cover splitting, and average bond strength values,
288 calculated considering only those specimens that failed following a pullout mode. Bond
289 strength values are shown for reference only. The variable subjected to analysis in the
290 following sections is the count of splitting cases, because this paper focuses on the
291 identification of variables that determine the mode of bond failure and the quantification
292 of their effect on splitting risk.

293

294 **5. ANALYSIS AND DISCUSSION**

295

296 **5.1 Development of a semi-empirical model to predict splitting risk**

297 Logistic binary regression [37] has been used to relate the probability (p) of cover
298 splitting in a POT specimen to the variables considered in this research (f_c , D , C , C_f , λ_f ,
299 l_f). This has been achieved by fitting a logistic equation to the experimental values
300 obtained for p , which can be 0/3, 1/3, 2/3, or 3/3, shown in Table 3.

301 In this case, a semi-empirical logistic model has been obtained, so that it takes into
302 account not only the experimental data obtained but also previous knowledge of bond

303 phenomena. This helps interpreting the implications of the relations modelled and
304 therefore adds value to the predictive tool.

305 This has been achieved by carefully pondering which interactions among the factors
306 considered are likely to be at operation in relation to bond failure. Before fitting a
307 logistic equation to the experimental data, the structure of this logistic equation has been
308 tailored so that it better represents bond phenomena. As explained in the introduction,
309 passive confinement plays a capital role on bond failure modes. If transverse
310 reinforcement is not considered (as it is the case in this research), concrete
311 cover/diameter ratio (C/D) is the main source of passive confinement. Therefore, it is
312 reasonable to think that C/D is the only factor having a standalone effect on the risk of
313 splitting, while its effect is modified by concrete properties. This implies the assumption
314 that all other factors (compressive strength, fibers content and geometry) interact with,
315 and therefore modify the effect of C/D ratio. This model is formulated by equation (1):

$$\ln\left(\frac{p}{1-p}\right) = \nabla_0 + (\nabla_{cd} + \nabla_c f_c + \nabla_{\mathcal{F}} C_f) \frac{C}{D} \quad (1)$$

316 where ∇_0 , ∇_{cd} , and ∇_c are coefficients to be estimated, and $\nabla_{\mathcal{F}}$ is a function of the
317 geometry of fibers defined as follows:

$$\nabla_{\mathcal{F}} = \nabla_f + \nabla_{\lambda_f} \lambda_f + \nabla_{\ell_f} \ell_f \quad (2)$$

318 where ∇_f , ∇_{λ_f} , and ∇_{ℓ_f} are coefficients to be estimated.

319 The model thus formulated takes into account the nature of the phenomenon under
320 study, and two aspects are particularly remarkable:

- 321 • The odds-ratio and therefore splitting probability are assumed to be mainly
322 determined by C/D ratio, and the effect of this factor is modified by a function
323 which depends on the properties of concrete, namely concrete compressive
324 strength (f_c) and fiber content (C_f). Under this light, fibers are understood to
325 modify the effect of C/D rather than having an effect of their own, assuming that
326 the effect of fibers is not independent from the degree of confinement in
327 geometrical terms or from concrete compressive strength.
- 328 • The effect of fibers is assumed to be mainly dependent on fiber content (C_f), but
329 the effect of fiber content is modified by means of a function which depends on
330 fibers geometry, $\nabla_{\mathcal{F}}$. This way, it is considered that the effect of fiber geometry
331 will depend on fiber content, which is a very reasonable assumption.

332 Estimated coefficients, together with the p-values obtained from the significance tests
333 on these estimates, are shown in Table 4. All the variables and interactions considered
334 in equations (1) and (2) have a statistically significant effect on the risk of splitting, as
335 shown by their p-values (not greater than 0.10 in any case).

336

337 **5.2 Semi-empirical model obtained to predict splitting failures**

338 If coefficients shown in Table 4 are introduced into equations (1) and (2), the final
339 model for splitting probability is obtained: equation (3) relates splitting probability to
340 the factors and interactions considered, and equation (4) presents the fiber geometry
341 function $\nabla_{\mathcal{F}}$ which modifies the effect of fiber content.

$$\ln\left(\frac{p}{1-p}\right) = 8.586 + (-12.63 + 0.219f_c + \nabla_{\mathcal{F}}C_f)\frac{C}{D} \quad (3)$$

342

$$\nabla_{\mathcal{F}} = -0.105 + 0.000325\lambda_f + 0.00174\ell_f \quad (4)$$

343

344 This model calculates values for the splitting probability p, but there is one last step so
345 that it can be used to predict splitting cases: a cutoff probability value p* has to be
346 established, so that situations where predicted p is p* or higher correspond to splitting
347 cases, while situations where predicted p are below p* correspond to no splitting cases.
348 The criterion to select this cutoff probability is based on classification efficiency: p*
349 value has to be selected so that the maximum percentage of splitting cases are correctly
350 predicted by the model. After trying different possibilities, the best option is p* = 0.5.
351 This means that predicted probabilities of 0.5 or higher correspond to splitting cases.
352 For all the combinations tested, the splitting probability is calculated and all
353 observations are sorted into two groups: splitting and no-splitting according to the
354 predicted p value. The classification obtained is shown in Table 5. It can be seen that
355 the fitted model proves highly accurate in terms of overall classification capacity
356 (95.1% of all cases are correctly predicted) and particularly in terms of correct
357 prediction of splitting failures (96% of all splitting cases are correctly predicted).

358

359

360

361

362 **5.3 Effect of compressive strength, C/D ratio and fibers content**

363 Figure 5 shows the values of splitting probability as predicted by the model –equations
364 (3) and (4)– versus C/D and C_f values. This will be referred to as the splitting
365 probability surface hereafter.

366 It can be observed that higher compressive strength values require higher C/D ratios for
367 splitting failure to be prevented. This can be interpreted as follows: when concrete
368 compressive strength increases, concrete tensile strength is increased and therefore
369 radial stresses developing around the rebar reach further away from it. In consequence,
370 it is more likely that tensile stresses reach the surface of the specimen, this meaning a
371 higher risk of splitting failure. As a result, higher concrete cover values are required
372 when concrete compressive strength is increased.

373 The horizontal plane in Figure 5 represents the cutoff probability set at $p^*=0.5$ for
374 classification purposes, which distinguishes splitting failures from pullout failures.
375 Accordingly, the intersection between this plane and the splitting probability surface
376 leads to the minimum concrete C/D values that are required to prevent splitting failures,
377 as shown in Figure 6. This requirement varies with fiber content.

378 The favorable effect of fibers when preventing splitting failures has been revealed to be
379 more important for higher compressive strength values. The reduction in the minimum
380 C/D ratio achieved when adding a certain fiber content to concrete is clearly bigger for
381 50-MPa concrete than for 35-MPa concrete, as seen in Figure 6.

382 There is another interesting remark to be made in relation to Figure 6. Since C/D of 5.0
383 is usually accepted as a good confinement situation, it follows that no splitting of
384 concrete cover should be expected. However, the validity of such an assumption is
385 restricted, as seen in Figure 6: according to the model developed, a POT specimen made
386 with 50-MPa concrete without fibers where C/D is 5.0 is likely to experience a splitting
387 failure.

388

389 **5.4 Effect of fibers geometry**

390 Figures 7 and 8 illustrate the effect of fibers content and geometry (slenderness in Fig. 7
391 and length in Fig. 8) together with C/D for a constant concrete compressive strength of
392 45 MPa.

393 Figure 7-left shows the splitting probability surface calculated for different values of
394 fiber slenderness for a fiber length of 50mm. The three splitting probability surfaces
395 shown in Figure 7-left are very close to each other. This points out that the effect of

396 fiber slenderness on the mode of failure of an anchorage, though statistically significant,
397 is not very important in magnitude. The intersection of these surfaces with the horizontal
398 plane $p^*=0.5$ leads to Figure 7-right, where minimum C/D values are shown for
399 different fiber contents and different values of fiber slenderness. It can be concluded
400 that low fiber slenderness values are preferred to prevent splitting of concrete cover.
401 The effect of fiber length on the mode of bond failure is more complex. Splitting
402 probability surfaces for different fiber length values, assuming a fiber slenderness of 65,
403 are shown in Figure 8-left. Contrarily to what has been observed concerning fiber
404 slenderness, splitting probability surfaces for different fiber length values are clearly
405 distinct. This clearly indicates that the effect of fiber length on the mode of failure of
406 anchorages, besides being statistically significant, is highly relevant. Figure 8-right
407 shows minimum C/D values required to prevent splitting failures after intersection of
408 surfaces in Figure 8-left with the horizontal plane $p^*=0.5$. It is observed that the
409 favorable effect of increasing fiber contents is conditioned to fiber length. The use of
410 long fibers can reverse the trends observed in Figures 5 and 6: when long fibers are used,
411 increasing the fiber content would make the anchorage more prone to splitting and
412 therefore higher C/D values would be required to prevent splitting failures. This would
413 be the case of 60-mm length fibers, as observed in Figure 8-right.

414

415 **5.5 Exploitation of the model: minimum cover/diameter ratios**

416 The model obtained, given by equations (3) and (4), fits very well the experimental data,
417 as explained in previous sections. However, some problems arise if this model is
418 generalized and extended to values of the different factors outside the range within
419 which they have been tested. This is illustrated in Figure 9, where the experimentally
420 fitted equation is plotted for concrete without fibers. The shaded region defines the
421 situations covered by the experimental results this model is based upon. In that case,
422 there is a vertical asymptote for a concrete compressive strength value of 57.7 MPa.
423 Therefore, the experimentally fitted equation is not valid for compressive strength
424 values higher than 50 MPa. This equation, however, can be modified to overcome this
425 difficulty.

426 One hypothesis that can be assumed is that the definition of good confinement provided
427 by the Model Code (FIB 2010) is a limit for splitting cases: a C/D value of 5.0 is always
428 enough to prevent splitting failures. If this condition is imposed to the experimentally
429 fitted equation, a continuous, smooth function can be proposed so that it best fits the

430 experimental curve and also the hypothesis arising from the Model Code [8]. This is
 431 shown in Figure 9 as "new equation", and for concrete without fibers it is as follows:

$$\frac{C}{D} = \frac{5 + \exp\left(\frac{f_c - 30}{3.8}\right)}{4.5 + 0.2\exp\left(\frac{f_c - 30}{3.8}\right)} \quad (5)$$

432 The same has been done for concrete with fibers. Figure 10 shows the curves
 433 generalized for different fiber contents, for $\nabla_{\mathcal{F}}C_f$ values between -2.0 and 2.0 (tested
 434 values are between -2.5 and 2.5) in addition to unfibred concrete ($\nabla_{\mathcal{F}}C_f = 0$). This
 435 generalized "new equation" is:

$$\frac{C}{D} = \frac{5 + \exp\left(\frac{f_c + 5\nabla_{\mathcal{F}}C_f - 30}{3.8}\right)}{4.5 + 0.2\exp\left(\frac{f_c + 5\nabla_{\mathcal{F}}C_f - 30}{3.8}\right)} \quad (6)$$

436 However, following Figures 9 and 10 it is clear that the assumption that a C/D value of
 437 5.0 is always enough to prevent splitting failures is not compatible with the
 438 experimental observations reported herein. The curves arising from equations (5) and
 439 (6), forced by the horizontal asymptote C/D = 5.0, are excessively diverging from the
 440 experimentally fitted equation within the region covered by this experimental
 441 programme. Taking into account that the predictive capacity of the model is very high
 442 (95.1%), these new formulations introduce an excessive reduction of the model's
 443 accuracy. Therefore, the hypothesis that a C/D = 5.0 should always suffice must be
 444 rejected because it is in contradiction with experimental results.

445 An alternative hypothesis can be considered: there might be a C/D value to prevent
 446 splitting failures in all cases, but this is not necessarily 5.0. Therefore, a continuous,
 447 smooth function other than (5) or (6) can be proposed as long as it meets the following
 448 two requirements: a) it must be consistent with the model obtained within the ranges
 449 covered by the experimental programme, and b) there must be a horizontal asymptote
 450 corresponding to a C/D value higher than 5.0.

451 Accordingly, the following equation is proposed, and it is plotted in Figure 11 for
 452 concrete without fibers and two cases of concrete with fibers:

$$\frac{C}{D} = 1.2 + \frac{(5.6 - 0.2\nabla_{\mathcal{F}}C_f) \cdot \exp\left(\frac{f_c + 5\nabla_{\mathcal{F}}C_f - 50}{5}\right)}{0.6 + 0.9\exp\left(\frac{f_c + 5\nabla_{\mathcal{F}}C_f - 50}{5}\right)} \quad (7)$$

453 As can be seen in Figure 11, it follows that the general limit that may be assumed for
454 cover/diameter ratio as well confinement would not be 5.0 but approximately 7.5,
455 although this value needs confirmation in the future by performing new tests.

456 Equation (7), together with equation (4) for the fiber geometry factor, is a generalized
457 form of the model obtained from experimental observations. This means that it is totally
458 valid within the ranges of values for the different factors tested in the experimental
459 programme, and it has the same accuracy than the model given by equations (3) and (4).
460 Furthermore, it presents no unreasonable discontinuities if it is generalized for values of
461 the factors considered that fall outside the experimental region, and therefore it is
462 adequate to be applied to values slightly different than the ones considered in the
463 experimental programme. However, its validity and accuracy outside this region has to
464 be checked by further experimental campaigns, especially regarding the absolute
465 threshold of $C/D = 7.5$ and the redefinition of the situation of good confinement from
466 $C/D = 5.0$ to $C/D = 7.5$.

467

468 **6. CONCLUSIONS**

- 469 • An accurate model for predicting the mode of bond failure has been developed.
470 It relates splitting probability to the values of concrete compressive strength,
471 rebar diameter, concrete cover, fiber content, fiber length, and fiber slenderness.
472 It has been verified that the margin of error is less than 5%.
- 473 • Higher compressive strength values require higher concrete cover/diameter
474 ratios for splitting failure to be prevented. When compressive strength of
475 concrete increases, concrete tensile strength is increased and therefore radial
476 stresses developing around the rebar reach further away from it.
- 477 • It has been proved that increasing fiber content reduces the risk of splitting
478 failure. The favorable effect of fibers when preventing splitting failures has been
479 revealed to be more important for higher concrete compressive strength values.
- 480 • Fiber slenderness and fiber length modify the effect of fiber content on splitting
481 probability and therefore on minimum cover/diameter ratios required to prevent
482 splitting failures.
- 483 • Higher fiber slenderness and/or fiber length values imply an increase in bond
484 capacity of concrete and therefore require higher concrete cover values to
485 prevent splitting when developing higher bond stresses.

- 486 • The favorable effect of increasing fiber contents is conditioned to fiber length.
487 The use of long fibers can even lead to the fact that increasing fiber contents
488 would make the anchorage more prone to splitting.
- 489 • It appears that the definition of the good confinement situations corresponding
490 to cover/diameter = 5.0, as established by the Model Code, is possibly
491 insufficient for SFRCs when concrete compressive strength higher than 50 MPa.
492

493 **ACKNOWLEDGEMENTS**

494 The authors of this work wish to thank both the Research Bureau of the Spanish
495 Ministry of Science and Innovation and the ‘Plan E’ programme for the funding of the
496 project ‘BIA 2009-12722’, this research being a part thereof.
497

498 **REFERENCES**

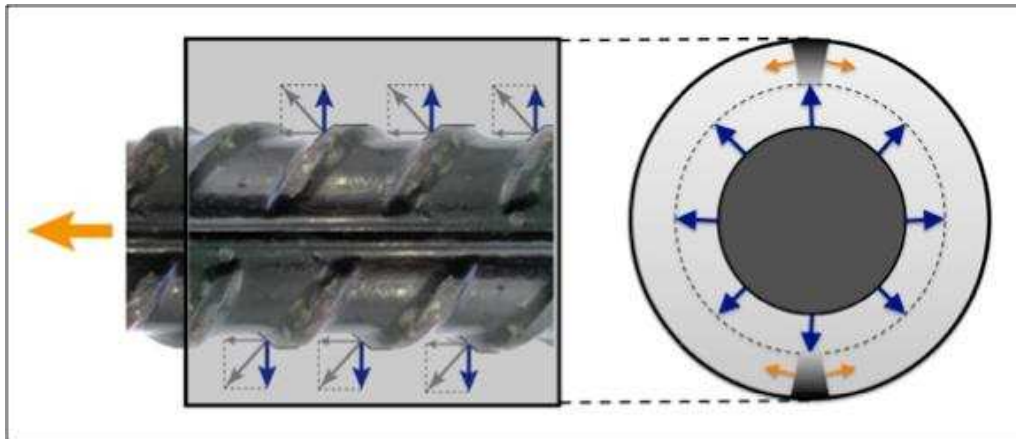
- 499 [1] Cairns J, Plizzari GA. Towards a harmonised European bond test. *Materials and*
500 *Structures* 2003;36:498–506.
- 501 [2] Bamonte PF, Gambarova PG. High-Bond Bars in NSC and HPC: Study on Size
502 Effect and on the Local Bond Stress-Slip Law. *Journal of Structural Engineering*
503 2007;133:225.
- 504 [3] Gambarova PG. Bond in reinforced concrete: where do we stand today?,
505 Proceedings of BOND2012 - Bond in Concrete 2012, Brescia, Italy: 2012, pp. 1–
506 13.
- 507 [4] Gambarova PG, Rosati GP, Zasso B. Steel-to-concrete bond after concrete
508 splitting: test results. *Materials and Structures* 1989;22:35–47.
- 509 [5] Bazant ZP, Li Z, Thoma M. Identification of stress-slip law for bar or fiber
510 pullout by size effect tests. *Journal of Engineering Mechanics* 1995;121:620–5.
- 511 [6] Bazant ZP, Sener S. Size Effect in Pullout Tests. *ACI Materials Journal*
512 1988;85:347–51.
- 513 [7] FIB–The International Federation for Structural Concrete. FIB Bulletin No. 10:
514 Bond of reinforcement in concrete. Lausanne, Switzerland, 2000, 434 pp.
- 515 [8] FIB–The International Federation for Structural Concrete. Model Code 2010.
516 Published by Ernst & Sohn, 2013, 434 pp.
- 517 [9] Cairns J, Jones K. The splitting forces generated by bond. *Magazine of Concrete*
518 Research 1995;47:153–65.

- 519 [10] ACI Committee 318, 2011. ACI 318-11: Building Code Requirements for
520 Structural Concrete and Commentary. Ed. by American Concrete Institute (ACI),
521 Farmington Hills, Michigan, United States, 503 pp.
- 522 [11] Yalciner H, Eren O, Sensoy S. An experimental study on the bond strength
523 between reinforcement bars and concrete as a function of concrete cover, strength
524 and corrosion level. *Cement and Concrete Research* 2012;42:643–55.
- 525 [12] Arel HS, Yazici S. Concrete-reinforcement bond in different concrete classes.
526 *Construction and Building Materials* 2012;36:78–83.
- 527 [13] García-Taengua E, Martí-Vargas JR, Serna-Ros P. Statistical Approach to Effect
528 of Factors Involved in Bond Performance of Steel Fiber-Reinforced Concrete.
529 *ACI Structural Journal* 2011;108:461–8.
- 530 [14] Cairns J, Plizzari GA. Bond behaviour of conventional reinforcement in fibre
531 reinforced concrete, Varenna, Italy: 2004.
- 532 [15] Holschemacher K, Weisse D. Bond of reinforcement in fibre reinforced concrete,
533 Varenna, Italy: 2004.
- 534 [16] García-Taengua E, Arango S, Martí-Vargas JR, Serna P. Flexural Creep of Steel
535 Fiber Reinforced Concrete in the Cracked State. *Construction and Building*
536 *Materials* 2014, DOI 10.1016/j.conbuildmat.2014.04.139
- 537 [17] Dancygier AN, Katz A, Wexler U. Bond between deformed reinforcement and
538 normal and high-strength concrete with and without fibers. *Materials and*
539 *Structures* 2010;43:839–56.
- 540 [18] Ministerio de Fomento, 2008. Instrucción Española de Hormigón Estructural
541 EHE-08, Madrid, Spain, 304 pp.
- 542 [19] ACI Committee 408, 2003. Report ACI 408R-03: Bond and Development of
543 Straight Reinforcing Bars in Tension. Ed. by American Concrete Institute (ACI),
544 Farmington Hills, Michigan, United States, 49 pp.
- 545 [20] Serna P, Arango S, Ribeiro T, Núñez A, García-Taengua E. Structural cast-in-
546 place SFRC: technology, control criteria and recent applications in Spain.
547 *Materials and Structures* 2009;42:1233–46.
- 548 [21] Shah AA, Ribakov Y. Recent trends in steel fibered high-strength concrete.
549 *Materials & Design* 2011;32:4122–51.
- 550 [22] Arango SE, Serna P, Martí-Vargas J, García-Taengua E. A Test Method to
551 Characterize Flexural Creep Behaviour of Pre-cracked FRC Specimens.
552 *Experimental Mechanics* 2012;52:1067–78.

- 553 [23] Darwin D, Zuo J. Development Length Criteria for Conventional and High
554 Relative Rib Area Reinforcing Bars. *ACI Structural Journal* 1996;93:347–59.
- 555 [24] Lundgren K, Gylltoft K. A Model for the Bond between Concrete and
556 Reinforcement. *Magazine of Concrete Research* 2000;52:53–63.
- 557 [25] Harajli MH, Mabsout ME. Evaluation of Bond Strength of Steel Reinforcing Bars
558 in Plain and Fiber-Reinforced Concrete. *ACI Structural Journal* 2002;99:509–17.
- 559 [26] Russo G, Pauletta M. A simple method for evaluating the maximum slip of
560 anchorages. *Materials and Structures* 2006;39:533–46.
- 561 [27] Russo G, Pauletta M, Mitri D. Solution for bond distribution in asymmetric R.C.
562 structural members. *Engineering Structures* 2009;31:633–41.
- 563 [28] Tastani SP, Pantazopoulou SJ. Direct Tension Pullout Bond Test: Experimental
564 Results. *Journal of Structural Engineering* 2010;136:731–43.
- 565 [29] Harajli MH. Bond Stress–Slip Model for Steel Bars in Unconfined or Steel, FRC,
566 or FRP Confined Concrete under Cyclic Loading. *Journal of Structural*
567 *Engineering* 2009;135:509–18.
- 568 [30] Cattaneo S, Rosati G. Bond between Steel and Self-Consolidating Concrete:
569 Experiments and Modeling. *ACI Structural Journal* 2009;106:540–50.
- 570 [31] Harajli MH, Hout M, Jalkh W. Local Bond Stress-Slip Behavior of Reinforcing
571 Bars Embedded in Plain and Fiber Concrete. *ACI Materials Journal* 1995;92:343–
572 54.
- 573 [32] RILEM-CEB-FIP, 1970. Bond test for reinforcing steel: 2. Pull-Out Test.
574 *Materials and Structures*, 3(3), pp.175–178.
- 575 [33] RILEM, 1983 (1994), RC6–Bond test for reinforcement steel. 2. Pull-out test.
576 *RILEM Recommendations for the Testing and Use of Constructions Materials*, pp.
577 218-220, ed. by E & FN SPON.
- 578 [34] Gambarova PG, Rosati G. Bond and splitting in reinforced concrete: test results
579 on bar pull-out. *Materials and Structures* 1996;29:267–76.
- 580 [35] EN 1992-1-1, 2004. Eurocode 2: Design of Concrete Structures – Part 1- 1:
581 General Rules and Rules for Buildings. Ed. by European Committee for
582 Standardization, Brussels, Belgium, 225 pp.
- 583 [36] Montgomery, D., *Design & Analysis of Experiments*, sixth edition, John Wiley &
584 Sons, Inc., New York, 2005, 643 pp.
- 585 [37] Kleinbaum, D.G., & Klein, M., 2010. *Logistic Regression: A Self-Learning Text*
586 (3rd ed.). Ed. by Springer, New Jersey, United States, 701 pp.

587 **FIGURES**

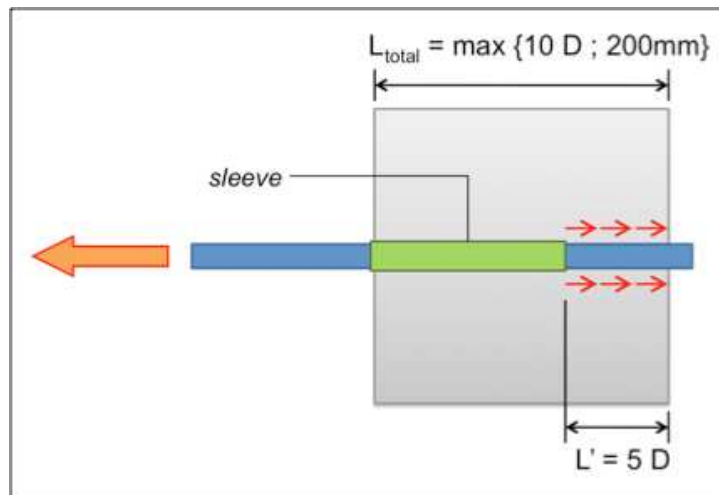
588



589

590 Figure 1. Bond stresses and radial stresses generated at the rebar-concrete interface.

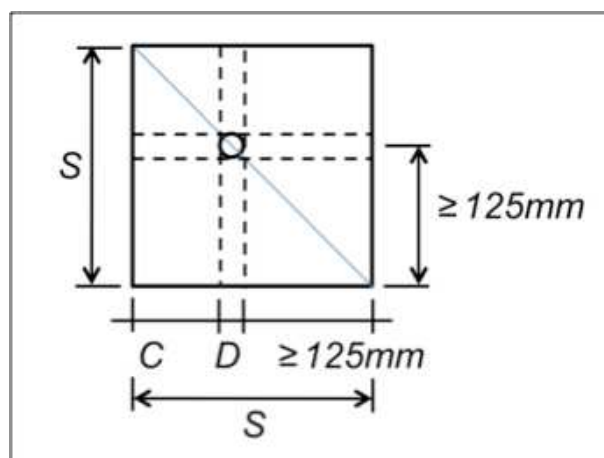
591



592

593 Figure 2. Longitudinal view of POT specimen according to RILEM recommendations.

594

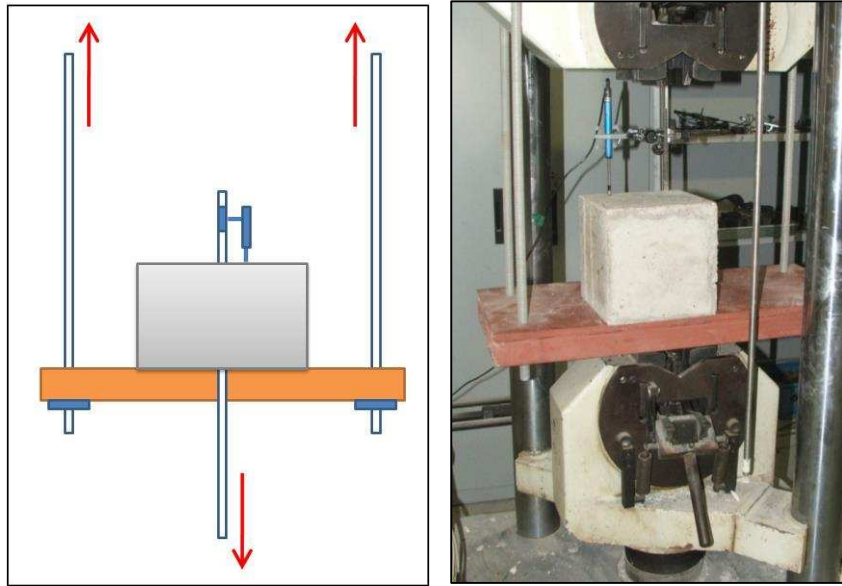


595

596

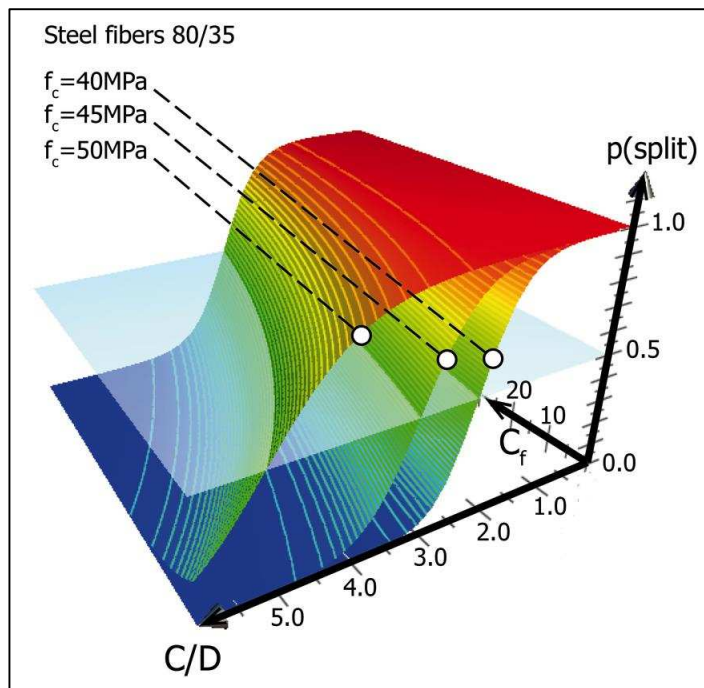
597 Figure 3. Cross-section of POT specimens.

597



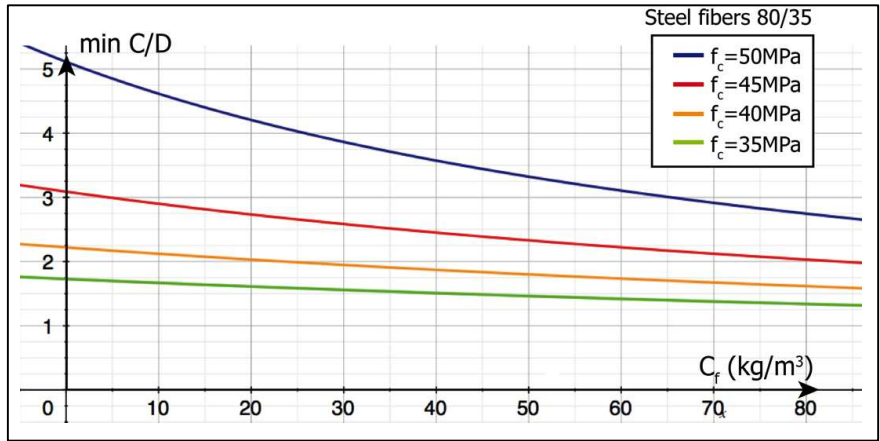
598
599
600
601

Figure 4. Force diagram (left) and a view of the pull out test as performed in this research (right).



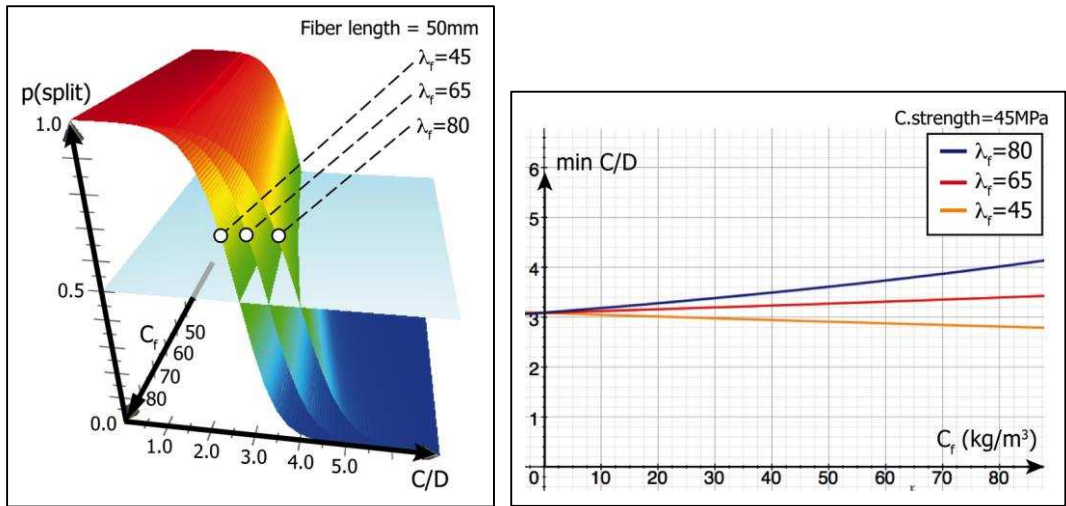
602
603
604
605

Figure 5. Splitting probability surfaces for concrete between 40MPa and 50MPa reinforced with 80/35 steel fibers.



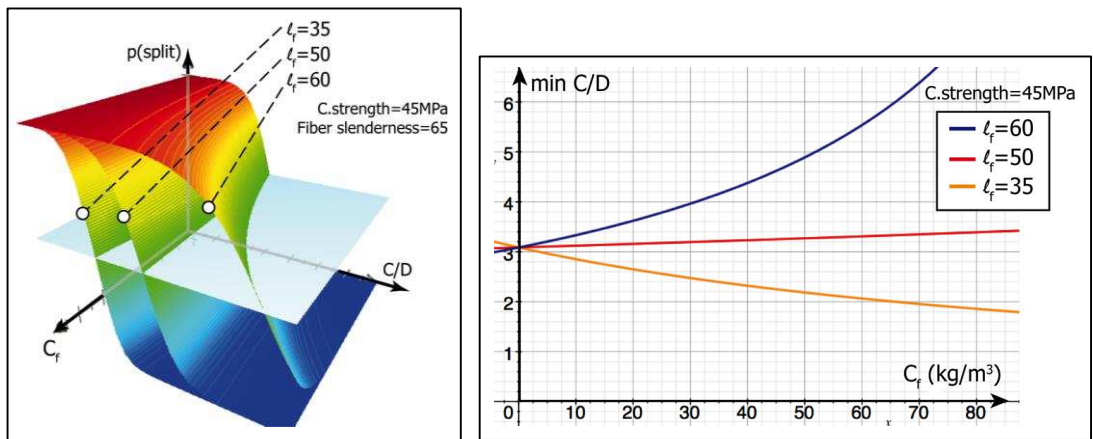
606
607
608
609

Figure 6. Minimum C/D values to avoid splitting failure of concrete reinforced with 80/35 steel fibers.



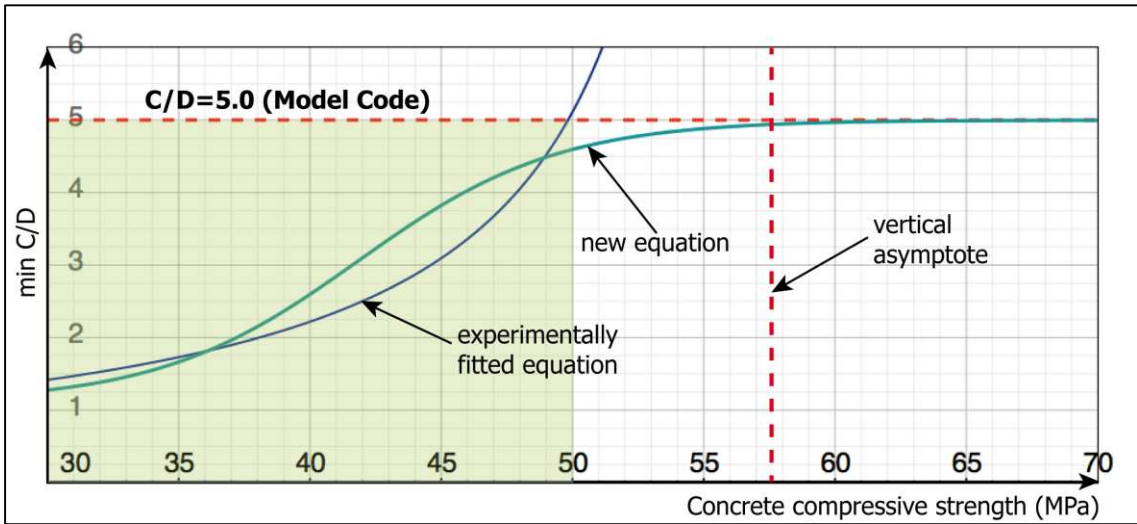
610
611
612
613

Figure 7. Splitting probability surfaces (left), and minimum C/D values to avoid splitting failure for 45-MPa concrete reinforced with 50-mm fibers (right).



614
615
616
617

Figure 8. Splitting probability surfaces (left) and minimum C/D values to avoid splitting failure, for 45-MPa concrete reinforced with fibers of slenderness 65.



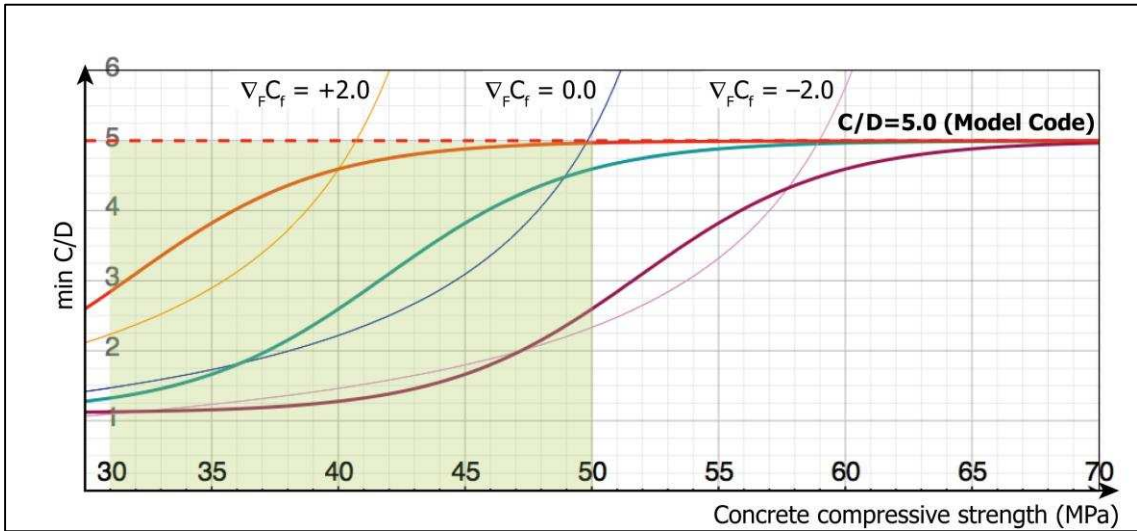
618

619

620

621

Figure 9. Function to relate min C/D to compressive strength (optimum C/D=5.0 according to Model Code)



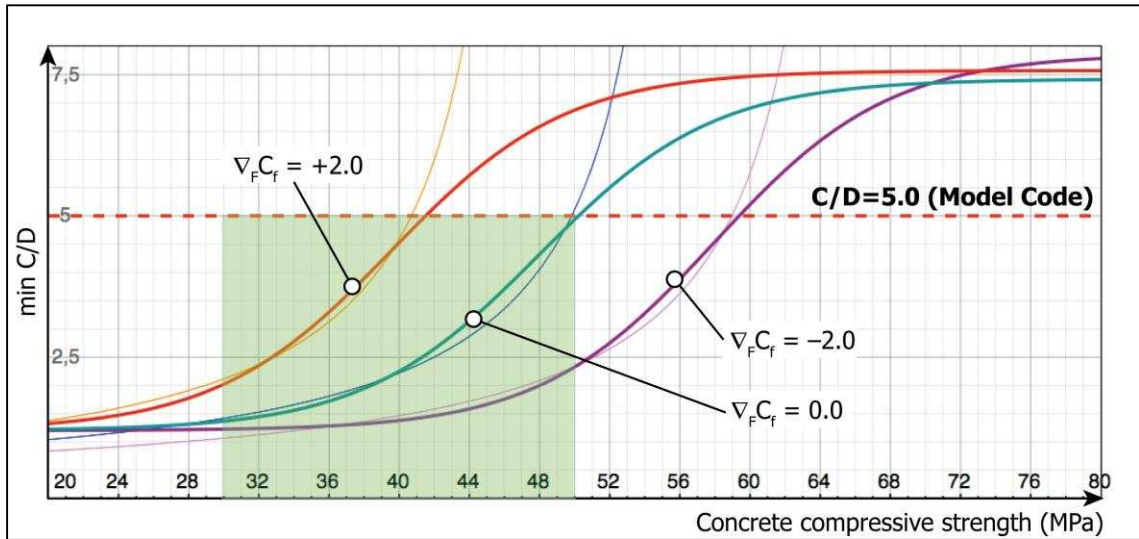
622

623

624

625

Figure 10. Generalized function to relate min C/D to compressive strength (optimum C/D=5.0 according to Model Code).



626

627 Figure 11. Generalized function to relate min C/D to compressive strength (Model Code
 628 optimum C/D=5.0 not assumed).
 629

630

630

631 TABLES

632

633

Table 1. Factors and levels considered.

	Type I mixes	Type II mixes	Type III mixes
Rebar diameter, mm	8 16 20	8 12 16	8 12 16
Concrete cover	C1=30mm C2=(C1+C3)/2 C3=5 D	C1=2.5 D C2=3.5 D C3=5.0 D	C1=2.5 D C2=3.5 D C3=5.0 D
Fiber geometry (slenderness / length)	65/60 80/50	45/50 80/50 80/35	45/50 80/50 80/35
Fiber content, kg/m ³	0 40 70	0 40 60	0 40 60

634

635

Table 2. Reference mix designs (kg/m³).

	Type I	Type II	Type III
Water/Cement	0.60	0.45	0.55
Cement	325	440	325
Sand 0/4	1006	957	1050
Coarse aggr. 7/12	544	723	835
Coarse aggr. 12/20	362	-	-
Filler	-	72	37
Superplasticizer	1.40	10	1.40

636

637

Table 3. Combinations tested and number of splitting cases observed.

Combination	Fibers geometry (λ_f / l_f)	Fiber content (kg/m ³)	Rebar diameter (mm)	Concrete Cover	Bond strength (MPa)	Splitting specimens
I-1	65/60	40	16	C1	6.24	0
I-2	-	0	8	C2	8.36	0
I-3	65/60	70	20	C3	18.44	0
I-4	65/60	40	8	C3	7.78	0
I-5	-	0	20	C1	--	3/3
I-6	65/60	70	16	C2	6.83	0
I-7	80/50	40	20	C2	11.79	0
I-8	-	0	16	C3	5.76	0
I-9	80/50	70	8	C1	5.62	0
II-1	-	0	8	C1	15.52	1/3
II-2	80/35	60	8	C2	31.12	0
II-3	45/50	40	8	C3	21.35	0

II-4	45/50	60	12	C1	--	3/3
II-5	80/50	40	12	C2	23.90	2/3
II-6	-	0	12	C3	25.29	0
II-7	80/35	40	16	C1	--	3/3
II-8	-	0	16	C2	--	3/3
II-9	80/50	60	16	C3	--	3/3
III-1	-	0	8	C1	--	3/3
III-2	80/50	40	12	C2	14.37	0
III-3	80/50	60	16	C3	21.95	0
III-4	-	0	12	C3	13.83	0
III-5	45/50	40	16	C1	--	3/3
III-6	45/50	60	8	C2	22.00	0
III-7	-	0	16	C2	21.15	1/3
III-8	80/35	40	8	C3	14.03	0
III-9	80/35	60	12	C1	20.98	0

638

639

640

Table 4. Estimated coefficients and significance tests for the semi-empirical model obtained for splitting probability.

		Coefficient	p-value
(constant)	∇_0	8.58577	--
Cover/Diameter, C/D	∇_{cd}	-12.629	0.0000
Compr. Strength, $f_c C/D$	∇_c	0.219206	0.0000
Fiber Content, $C_f C/D$	∇_f	-0.105321	0.0004
Fiber Slenderness, $\lambda_f C_f C/D$	∇_{λ_f}	0.00032465	0.0799
Fiber Length, $\ell_f C_f C/D$	∇_{ℓ_f}	0.0017429	0.0003

641

642

Table 5. Classification table, threshold probability of 0.5 (semi-empirical model).

Observed		Predicted		Percentage correct
		pullout	splitting	
pullout	56	53	3	53/56= 94.6%
splitting	25	1	24	24/25= 96.0%
Total: 56 + 25 = 81 specimens				overall (53 + 24)/81= 95.1%

643

644